Cross-Spectral Phase Method for Distinguishing Waves from Turbulence in Single-Point Boundary Layer Flow Measurements

Weichang Li and Albert J. Williams 3rd
Woods Hole Oceanographic Institution
98 Water St. MS#12
Woods Hole, MA 02543 USA

Abstract- **Cross-spectral analysis was applied to fixed single-point current measurements obtained using a Modular Acoustic Velocity Sensor (MAVS) from a shallow deployment in a tidal channel in Vineyard Sound south of Woods Hole, Massachusetts. Distinct phase signatures at different frequency bands were found in the cross power spectra between the vector components of velocity and between velocity and pressure. Velocity and pressure data had been obtained in burst samples both during periods when the flow was dominated by tidal currents and during periods when the flow was dominated by surface waves. Our analyses show that the phase signature in the cross power spectra can be used to effectively separate waves from turbulence over a broad range of scales that we sampled. In addition, the phase signature of the Cartesian velocity components has been derived in terms of the acoustic axes that comprise the raw measurements of velocity from MAVS. This association is used to distinguish between turbulence contributions and electronic noise at the intermediate to high frequency bands. By separating flow fluctuations due to turbulence from those due to waves a more accurate and representative observation of boundary layer dynamics can be obtained from a single-point vector flow measurement in the bottom boundary layer. Where these bands can be separated in frequency, Reynolds stress as well as structural eddies can be distinguished from waves.**

I. INTRODUCTION

Boundary layer fluid friction is mediated by turbulent eddies that transport momentum from the mean flow to the boundary. This is Reynolds stress, a negative correlation of fluctuations in the downstream velocity with fluctuations in velocity normal to and away from the boundary or upward for a simple horizontal planar bottom. This stress is theoretically a spatial average over a plane parallel to the boundary with a linear dimension many times the distance of the plane from the boundary, but in practice the average is taken not over a plane but at a single point over a duration in time that is long compared to the passage of an individual eddy but short compared to the variations in the mean flow strength. This substitution of temporal average for spatial average requires that the flow be steady and homogeneous, that it satisfies the ergodic hypothesis, a situation that is rarely strictly true. If there is an influence of surface gravity waves present in the bottom flow, a periodic reversal of flow direction or at least a modulation of flow magnitude, the structure of the boundary layer is more complex because the flow is certainly not steady.

While the instantaneous velocity close to the boundary would seem to be the quantity responsible for bottom stress and friction between the flow and the boundary, it is not so simple since it takes time for the eddies to form and the wave boundary layer within which such eddies do form is very thin, much thinner than can be observed with standard velocity sensors. Consequently, wave boundary layer eddies may suspend sediment from the bottom but do not determine the total boundary layer stress. However, the reversal or modulation of flow velocity in the bottom boundary layer does make observation of Reynolds stress difficult. Thus wave velocities must be identified and separated from turbulence before this Reynolds stress estimate can be made.

Vector velocity measurements of current at a fixed single point near the bottom can measure attenuated surface wave orbits and horizontal velocity measurements combined with pressure measurements can measure surface waves even when the sensor is so close to the bottom that the vertical component of wave velocity is nearly zero [1, 2]. Analysis programs exist to project such near bottom measurements back to the surface for directional wave spectra, useful for surface vessel navigation [3]. Mixing and transport processes, sediment transport for example, are strongly influenced by near bottom flow, both wave-induced and turbulent. Vector velocity sensing can provide temporal characteristics of such flow at a point over applicable periods. On the other hand, the extraction of information from the recorded data is complicated by the mix of generating mechanisms. For instance, the separation of surface waves from turbulence has been a long standing problem [4]. Also, noise can impact the calculation of mean turbulence parameters [5, 6].

The Modular Acoustic Velocity Sensor (MAVS), a three-axis acoustic differential travel-time point sensor, provides vector velocity measurements within a small volume [7]. MAVS has been successfully deployed to measure the directional wave spectrum [1] and turbulence [8], and, as part of a large marine observatory, to monitor waves and current [2]. Spectral analysis has been routinely applied to process the measured velocity data and compute the associated power spectrum. The cross power spectra between individual velocity components and between velocity and pressure have been used to construct the directional wave spectrum [1, 3]. However, in these analyses only the magnitudes of the spectral information, *i.e.* the cross power spectral density and the coherence, are retained. Yet under periodic motion caused by surface waves the phase lags between the individual velocity components and between velocity and pressure fluctuations are known. Momentum carrying eddies responsible for Reynolds stress also have known phase relationships between vector components of flow. Turbulent vortices shed by supporting structures in a tripod near the sensor have known phase relationships. These phase relationships are generally distinct and may take place in various frequency bands as a result of the flow being generated by different mechanisms. This phase signature information can potentially be used to separate waves from turbulence and possibly vortex shedding from Reynolds stress.

II. Description of Experiment

Velocity Sensor and MAVS Tripod

Two rings support eight acoustic transducers defining four acoustic axes along which the flow velocity is measured. Each acoustic axis is inclined 45º to the horizontal and spaced 90º in azimuth. In the experiment presented here, the sensor was pointed down and MAVS was mounted on the upper vertex of a short tripod with the sensor in relatively clear flow in the center of the enclosed volume as shown in Fig. 1. Each transducer of a pair produces a 1.8 MHz acoustic burst of 16 cycles and the received signals at the opposite members are compared where the difference in travel time is measured and stored. Each transmission is repeated with the transducers electrically reversed and the two measurements of differential travel time are subtracted to remove drifts and biases. The electronic noise in each measurement is equivalent to 0.05 cm/s with a long-term zero velocity uncertainty of 0.3 cm/s (absolute offset when immersed in still water).

Since the acoustic paths are spaced around the ring and inclined, each path is most sensitive to fluctuations in velocity along the acoustic axis and thus most sensitive to vortices shed by the closest upstream leg of the tripod. Fig. 2 shows the rings of the sensor schematically with the four acoustic axes that are combined to give Cartesian velocity vector components, U, V, and W. Electrical or vortex induced noise in one acoustic axis affects all three Cartesian components of flow so, before combining them, the sensitivity of each axis must be analyzed. When examined during periods of slack tide, all acoustic axes have a low spectral level except at surface wave frequencies as shown in Fig. 3. Thus the electronic noise in this deployment is negligible compared to flow noise. When the current flows westward (ebb), spectral levels for axes A and B are elevated over axes C and D for frequencies above 0.1 Hz (Fig. 4). By contrast, during eastward flow (flood), axes C and D are elevated over axes A and B above 0.1 Hz (Fig. 5). The affected pairs of axes are those in a plane parallel to the upstream leg of the tripod. Vortex generation from a sloping cylinder apparently has maximum energy in a plane including the cylinder but inclined to the angle of the cylinder (perpendicular to the plane of downstream vector and cylinder but including the cylinder). This result is surprising and not covered in classical treatment of the von Kármán vortex street, a two dimensional treatment. However, the frequency band where the energy is elevated confirms that there is vortex shedding from a cylinder 8 cm in diameter, essentially that of the tripod leg.

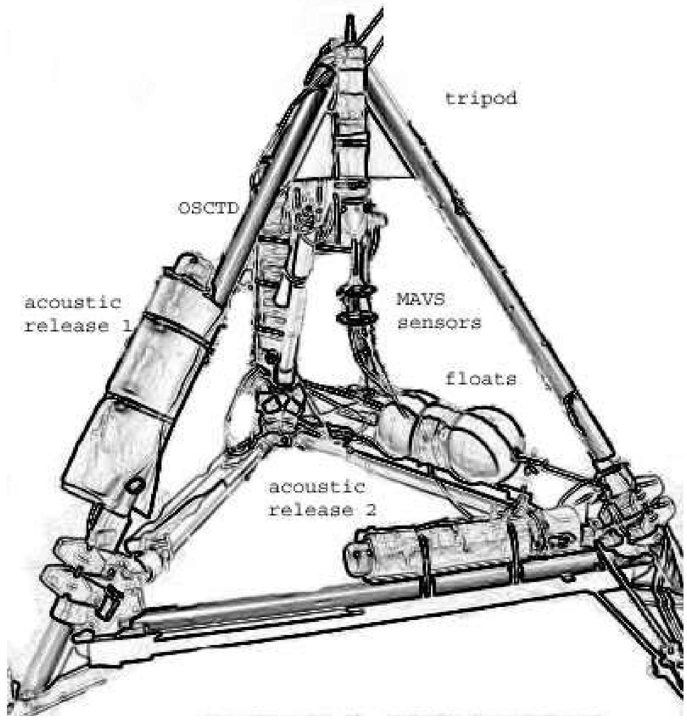

Fig. 1. The tripod from which the measurements were made is 1.66 meters tall and 2.13 meters between the feet with 6.4 cm struts to the apex where a MAVS (Modular Acoustic Velocity Sensor) current meter was mounted with the sensor rings defining the measurement volume positioned 0.74 meters above the base. Eastward tidal flow (flood) is directly into the page with minimum flow disturbance while westward tidal flow (ebb) comes to the sensor after passing near the distant tripod leg, thickened by a CTD sensor strapped to the leg.

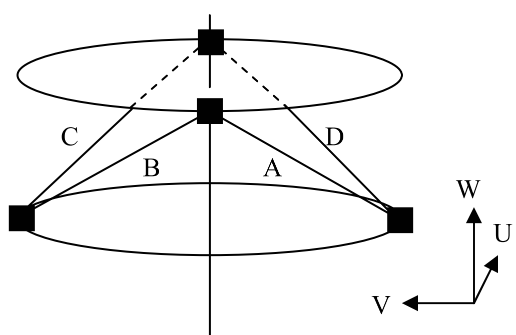

Fig. 2. The schematic representation of the velocity sensor of MAVS indicates the four acoustic axes labled A, B, C, and D. The axes are all inclined 45º to the horizontal and spaced 90º in azimuth. The direction into the plane of the figure as in Fig. 1 is the positive U direction. Tidal flood current to the east (U direction) enters the relatively open face of the tripod. Tidal ebb current to the west (-U direction) passes over the distant tripod leg.

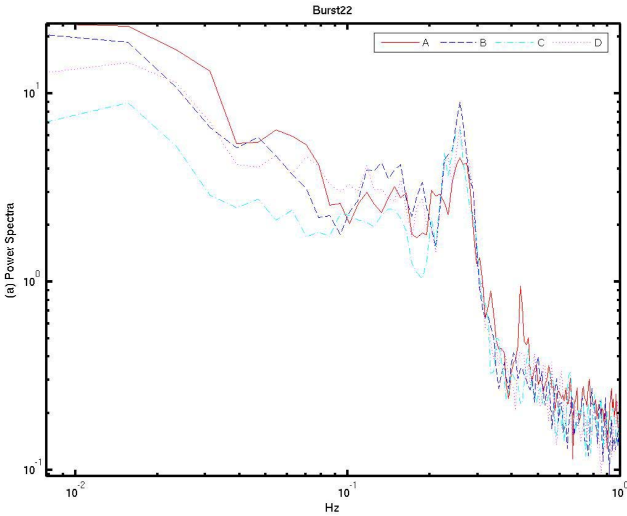

Fig. 3. The power spectra of the four acoustic axes from burst 22 where the tidal current was slack shows that only waves were present. At 1 Hz the power for all acoustic axes is below 0.3 $(cm/s)^2/Hz$.

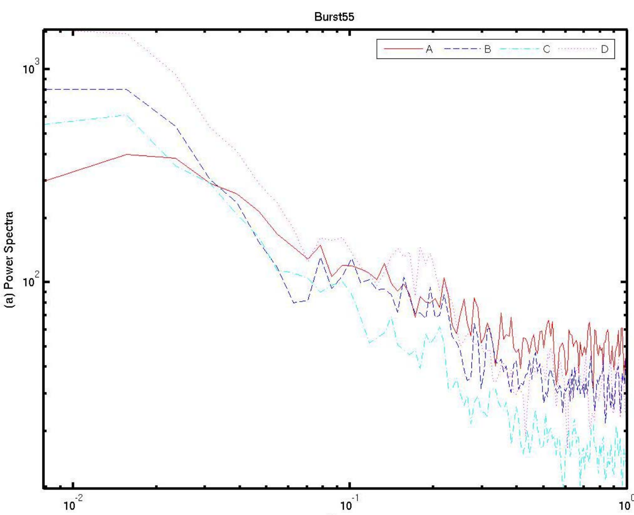

Fig. 4. The power spectra of the four acoustic axes from burst 55, a strong westward flow varying from 20 cm/s to 55 cm/s over the burst duration of 34 minutes, shows elevated power in axes A and B from 0.3 Hz to 1 Hz. Power for C and D remain as in Fig. 3 while A and B are as much as 40 $(cm/s)^2/Hz$ while C and D are a third as high. For westward flow, as in this example, vortex shedding by the upstream tripod leg generates turbulence in the plane of the A and B acoustic axes. The frequencies where the power is elevated are those for an 8·cm diameter cylinder with flow velocities between 20 and 60 cm/s.

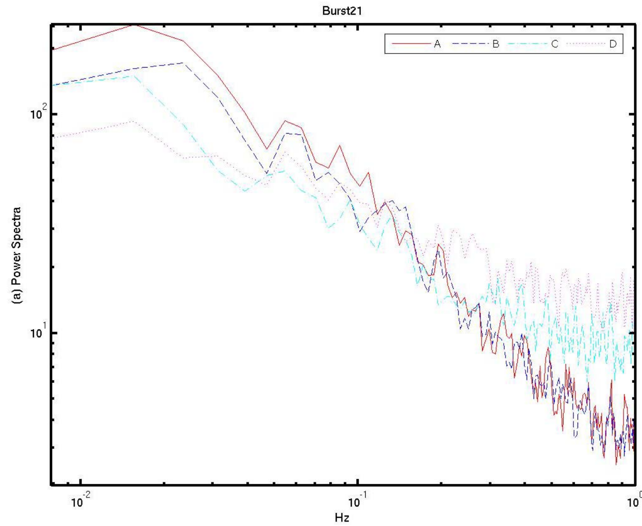

Fig. 5. The power spectra of the acoustic axes for eastward flow in burst 21 shows elevated levels for axes C and D. Although the tripod is relatively open for flow in this direction, tripod legs upstream of the sensor are inclined in the plane of axes C and D and this appears to cause elevated power in the vortices that are sensed by these axes. Frequencies, spectral levels, and velocities are similar to those affecting axes A and B in Fig. 4.

Sampling Frequency and Burst Sampling

MAVS sampled all four acoustic axes every 500 ms (2 Hz rate) in an interval of 15 ms. Spectra extend to 1 Hz, the Nyquist frequency, and include the frequencies of waves, vortex shedding from the tripod legs, and the eddies that contribute to Reynolds stress. In each burst, 4096 samples were taken for efficient spectral analysis, the burst length of 34 minutes being sufficient for spectral resolution of surface gravity waves. The bursts were repeated every 2 hours in order to observe conditions at varying stages of the tidal flow and wave generating events. Fig. 6 shows the time series of MAVS velocity measurements and of the temperature and salinity from the Oceans Sensors internally recording CTD positioned on the far leg of the tripod shown in Fig. 1.

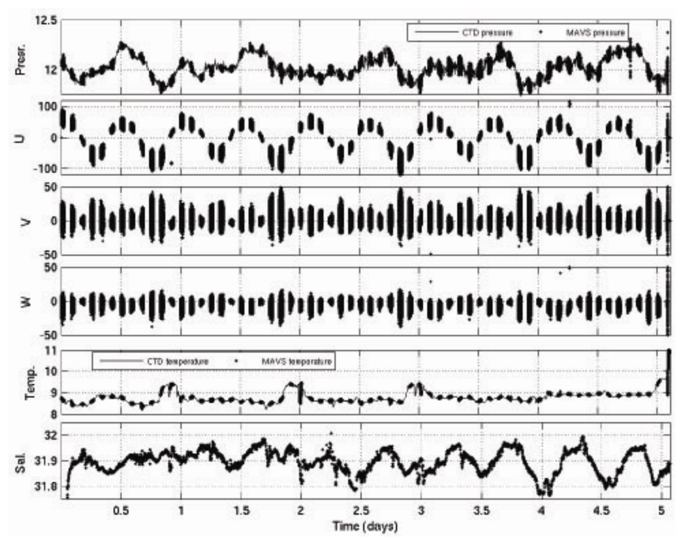

Fig. 6. The time series of current meter data and CTD data for the deployment of 5 days is shown in six panels. Each burst of velocity components shows the range but the individual values cannot be resolved. In this treatment, U is downstream for easterly tidal flow (flood) and –U is downstream for westerly tidal flow (ebb). V is cross stream, approximately north, and W is vertical up. Pressure is decibars or meters of depth at 0.85 m above bottom. Ocean Sensors CTD data is continuous while MAVS temperature and pressure are plotted on top as bursts.

Catalog of Bursts

Bursts 2 through 63 are shown in Fig. 6. Burst 21 was selected for an example of strong tidal flood (U positive) as shown in Fig. 3 while burst 55 was selected for strong tidal ebb (U negative) as shown in Fig. 4. Although waves are present in both of these cases the wave velocities are small in comparison to the mean and turbulence velocities. Burst 22 occurred during slack before ebb with waves present and represents almost pure wave velocities. Finally, burst 16 (Figs. 7 and 8) represents the class of waves with weak flow, flood in this case. A distinction is made between flood and ebb because of the dominant vortex contribution of the distant tripod leg in Fig. 1 for ebb.

Burst 16 illustrates the plain power spectra for this mix of relatively undisturbed flood tidal current and waves. Fig. 7 shows power spectral levels of streamwise coordinates of velocity, U, V, and W, and of pressure. Note that the pressure spectrum reveals two dominant wave frequencies of 0.147 Hz (7 s wave) and 0.21 Hz (4.7 s wave). There is even a lower amplitude pressure peak with frequency 0.25 Hz (4 s wave) representing the local wind driven sea on top of a long period swell coming down Vineyard Sound from the open ocean.

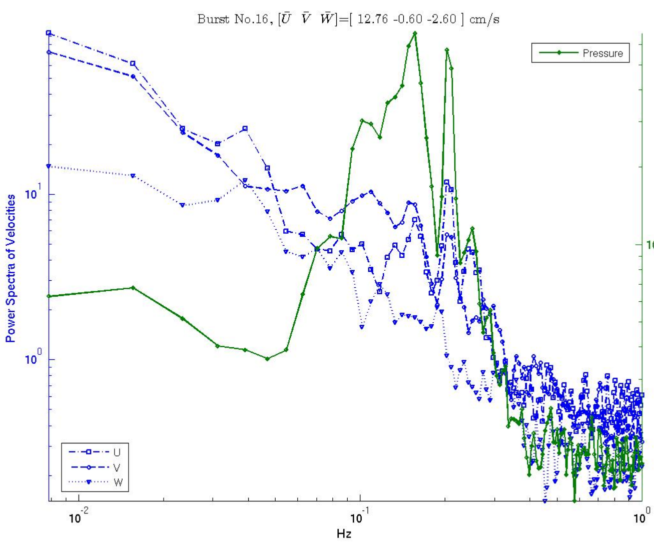

Fig. 7. Power spectra of streamwise (U), cross stream (V), and vertical (W) components of velocity [(cm/s) ^{2}/Hz] with power spectrum of pressure [(decibars) ^{2}/Hz] are shown for burst 16. This burst was taken during weak tidal flood with waves of 7, 5, and 4 s period.

III. Cross Power Spectral Analysis

The phase between the vertical velocity and the wave propagation direction velocity is 90º in surface gravity waves. If the wave propagating direction is U, then W is 90º retarded from U. Pressure, P, is in phase with U. In this treatment, U is east and defined as positive for flood tidal current. When cross spectra are calculated for waves, the directions may not be those of the wave orbits since the wind generated waves may be southerly although the swell may be easterly. As a consequence, a wave propagating to the south will have the pressure and V component of velocity 180º out of phase and the phase relation between P and U will be poorly defined in the wave band. An example is shown in Fig. 8 for burst 16 where there was swell propagating to the east (positive U) and higher-frequency wind-generated sea propagating to the west.

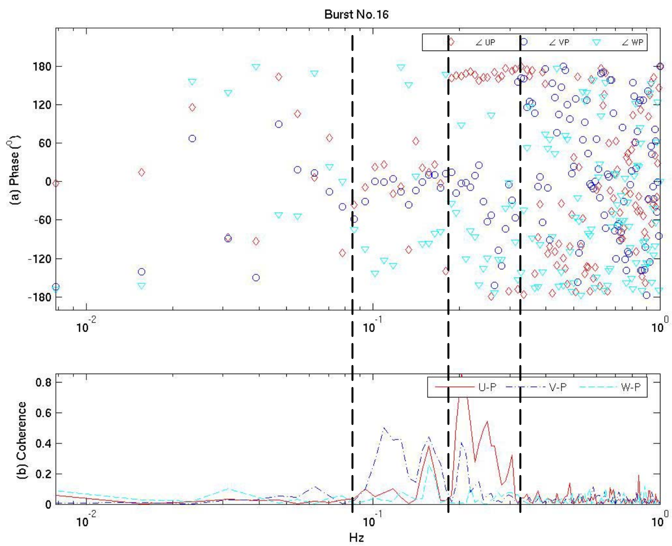

Fig. 8. The cross spectra from burst 16 of Fig. 7 shows the phase of U and P to be 180º out of phase in the band 0.2 Hz to 0.3 Hz. This is consistent with a wave propagating in the negative U direction. In the band from 0.1 Hz to 0.2 Hz, the phase between U and P is 0º but that between V and P is 180º. These phase relations are consistent with one long period wave propagating eastward and another propagating southward.

While Fig. 8 illustrates the phase relations between pressure and velocity components east and north (either 0° or 180° depending on the wave propagation direction relative to the tidal flow coordinates), the relation between horizontal wave velocity and vertical wave velocity is 90° out of phase. This is illustrated for burst 16 in Fig. 9. Since the vertical component of the wave velocity, W, is measured only 0.74 m above the bottom in 11 m depth, the vertical orbital wave velocity is small and the correlation for phase between U and W and between V and W is much less that that for the correlation between U and P and between V and P. However, the 5 s wave is clearly indicated by the +90° phase relation between U and W and by the -90° phase relation between V and W in the figure.

Fig. 10 illustrates the 90° phase relation between U and P and between V and P for the waves-only case of burst 22 shown in Fig. 3.

Cross Power Spectra of Turbulence

During burst 21 where the flow was strongly eastward (positive U) and into the relatively open face of the tripod, there is a low frequency phase signature of turbulent eddies, the type that can mediate Reynolds stress contributions to bottom friction. Fig. 11 shows the cross power spectra of UW and of VW in this burst, represented in Fig. 5 by the power spectra of the individual acoustic axes. There are high-frequency in-phase signatures as well, possibly caused by vortex shedding from upstream legs of the tripod. Since these eddies are not generated by a horizontal plane as are the Reynolds stress eddies, they do not have the phase relation of 180° as the low frequency eddies do. There are several peaks in UW coherence at 0.6 Hz, 0.7 Hz, 0.8 Hz, and 0.9 Hz. These appear to be related to the vortex shedding of the tripod legs.

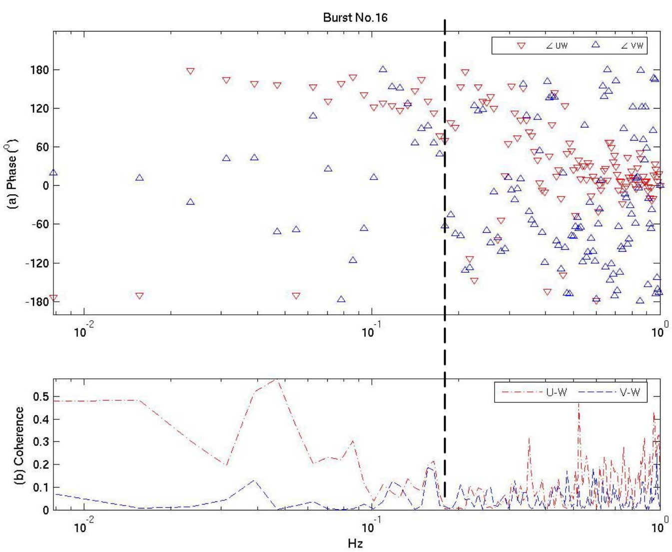

Fig. 9. The phase between U and W and between V and W in a wave is 90°. This is illustrated for the 5 s (0.2 Hz) wave from burst 16 illustrated in Fig. 7. The coherence is low because W associated with the wave is small so near the bottom and is masked by other motions.

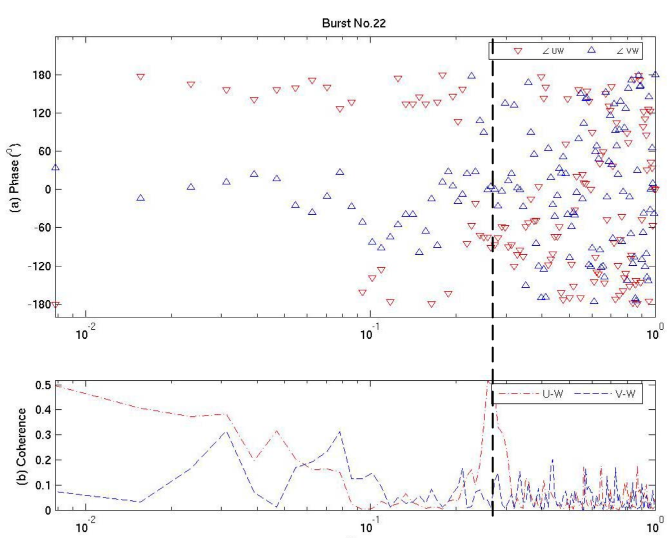

Fig. 10. The 90° phase between U and W is shown for the wave-only case of burst 22 shown in Fig. 3. The coherence is reasonable at the wave frequency of 0.25 Hz (4 s).

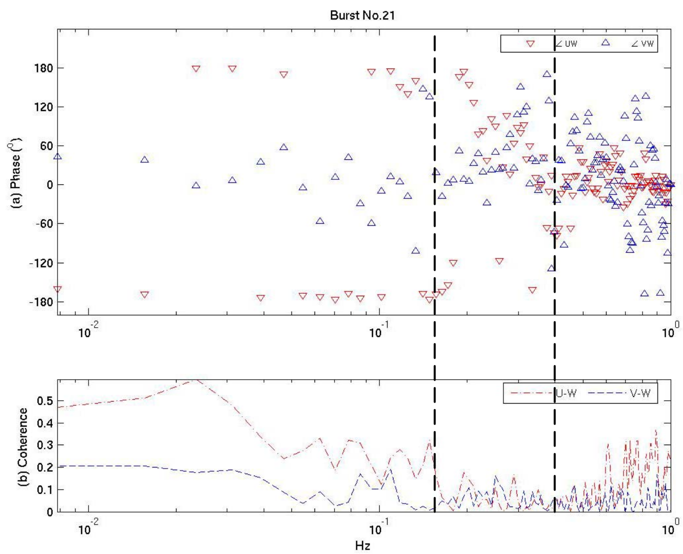

Fig. 11. The phase between U and W for burst 21 shown here is 0° for frequencies above 0.4 Hz. This is also the frequency band where acoustic axes A and B show elevated power, presumed to be due to vortex shedding by the upstream legs of the tripod that lie in the same plane as the axes. At frequencies below 0.15 Hz, the phase of the UW cross power spectrum is 180°, consistent with Reynolds stress eddies where ‘sweeps’ consist of negative W fluctuations correlated with positive downstream fluctuations in velocity. Ejective ‘bursts’ are positive W fluctuations correlated with negative downstream fluctuations. There are only weak cross power spectral signatures in the cross flow (V) direction.

The time series of velocity during burst 55 shows variations between 20 cm/s and 55 cm/s while the scale and period of Reynolds stress type eddies is expected to be highly variable. Since the sweep and burst character of the momentum transporting eddies is inherently episodic and intermittent at a point in space, the process appears to be broadband as the extended range of high coherence for UW from 0.04 Hz to 0.008 Hz indicates.

Cross Power Spectra of Vortex Shedding by Tripod Leg

Contamination of velocity measurements by an upstream tripod leg occurs with westward mean current. Burst 55 is an example, the acoustic axes of which were shown in Fig. 4. Streamwise and cross stream coordinate power spectra are shown in Fig. 12. Elevated power in V (cross stream) over the downstream U suggests vortex shedding in this case.

As in the eastward current case of Fig. 11, the vortices shed by the leg are at a higher frequency than the waves or the eddies associated with Reynolds stress and can be discarded in the treatment of the boundary layer flow. Fig. 12 shows the cross power spectra of UW and VW for this case. Since the current is strongly to the west and U is defined not as a streamwise direction but as east, the flow is negative and the correlations of fluctuations between U and W would be negative except for this flow direction reversal. This is indicated by 0º phase shift for the UW angle below 0.25 Hz. The coherence for UW correlations increases towards lower frequency while the phase remains 0º.

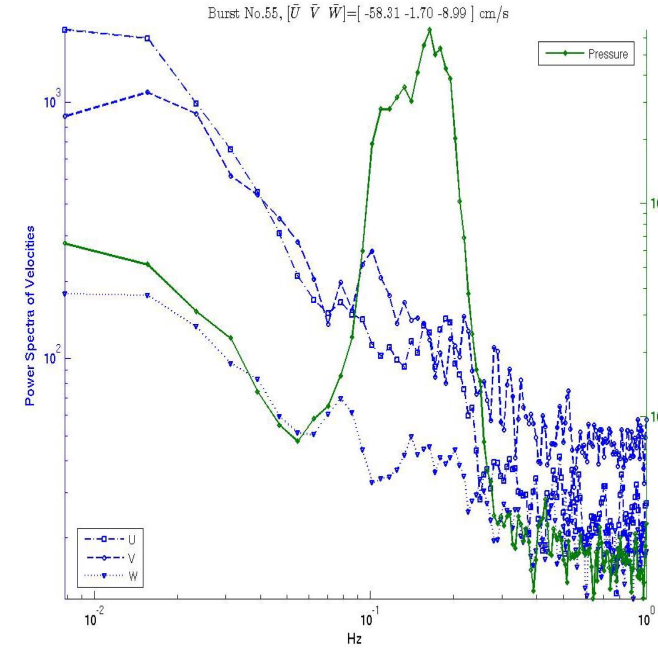

Fig. 12. With the strong westward current (-U) of burst 55 shown in Fig. 4, the upstream leg shown in Fig. 1 generates vortices that elevate the power spectral level of V, the cross stream axis, over U, the downstream axis.

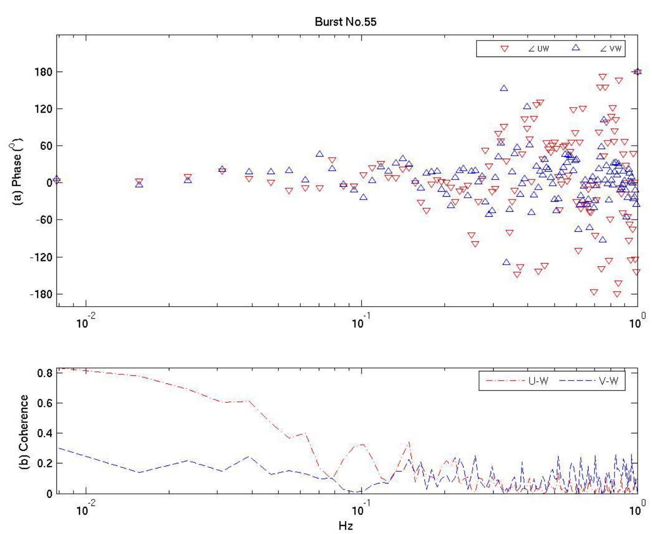

Fig. 13. Vortex shedding by the upstream leg of the tripod visible in Fig. 1 during burst 55 shown in Fig. 12 gives low coherence and variable phase to the cross power spectra above 0.25 Hz. However at lower frequencies the coherence for UW increases and the phase is 0º which is consistent with Reynolds stress mediating eddies (since U is positive for east flow and this is west flow and thus negative U).

IV. Conclusions

Vector measurements of flow near the bottom in shallow water with a fixed single-point current sensor can identify waves, Reynolds stress eddies, and turbulence generated by structures in the upstream direction. Spectra alone are helpful in separating the frequencies for waves from those for turbulence but cross power spectra allow the eddies of turbulence to be distinguished from the orbital motion of waves, even when they occupy the same bands. Vortices from an upstream tripod leg do not show the same phase as eddies from a horizontal plane and can be distinguished in the cross power spectra , even when the total power spectra are unable to do so.

V. Acknowledgements

The WHOI/MIT Joint Education Program provided teaching support for Williams and ship time on R/V *Tioga* for the deployment and recovery of the instrument package that gathered the data for this treatment. Jim Irish and the members of the 2004 Oceanographic Instrument Systems class are thanked for their assistance. Li was supported by a graduate research assistantship from Woods Hole Oceanographic Institution.

References

[1] A.J. Williams III and E.A. Terray, "Measurement of directional wave spectrum with a modular acoustic velocity sensor," *Oceans 2000,* 2000, IEEE Cat. No. 00CH37158, pp. 1175-1180.

[2] A.J. Williams III, J.J. Fredericks, E. Hobart, M,S. Carson, C. Tierney, and A. Waterbury, "Observatory measurements of waves and current," Proc. of the IEEE/OES 7th Working Conference on Current Measurement Technology, March 2003, IEEE Cat No. 2003CH37444, pp 257-263.

[3] A.T Morrison III, "MWAVES - Software for calculating the directional spectra and statistical properties of the wave field from MAVS-3 triplet measurements," Proc. of the IEEE/OES 7th Working conference on Current Measurement Technology, March 2003, IEEE Cat No. 2003CH37444, pp. 128-134.

[4] J.H. Trowbridge, "On a technique for measurement of turbulent shear stress in the presence of surface waves," J. Atmos. Oceanic Technol., vol. 15, pp. 290–298, 1998.

[5] R.G. Voulgaris and J.H. Trowbridge, "Evaluation of the Acoustic Doppler Velocimeter (ADV) for turbulence measurements," J. Atmos. Oceanic Technol., vol. 15, pp. 272–289, 1998.

[6] D. Hurther and U. Lemmin, "A correction method for turbulence measurement with a 3D Acoustic Doppler Velocity Profiler," J. Atmos. Oceanic Technol., vol. 18, pp. 446–458, 2001.

[7] F.T. Thwaites and A.J. Williams III, "Development of a modular acoustic velocity sensor," *Oceans 96*, 1996, IEEE Catalog Number 96CH35967, pp. 607-612.

[8] P.J. Hendricks, "Comparison of turbulence measurements from a SonTek ADV and a Nobska MAVS," *Oceans 2001*, 2001, IEEE Cat. No. 01CH37295, pp 1860-1866.